Photochemical & Photobiological Sciences
https://doi.org/10.1007/s43630-024-00573-y

ORIGINAL PAPERS

Near-infrared two-photon absorption and excited state dynamics of a fluorescent diarylethene derivative

Hikaru Sotome[1] · Tatsuhiro Nagasaka[1] · Tatsuki Konishi[2,3] · Kenji Kamada[2,3] · Masakazu Morimoto[4] · Masahiro Irie[4] · Hiroshi Miyasaka[1]

Received: 13 November 2023 / Accepted: 4 April 2024

Abstract

Near-infrared two-photon absorption and excited state dynamics of a fluorescent diarylethene (fDAE) derivative were investigated by time-resolved absorption and fluorescence spectroscopies. Prescreening with quantum chemical calculation predicted that a derivative with methylthienyl groups (mt-fDAE) in the closed-ring isomer has a two-photon absorption cross-section larger than 1000 GM, which was experimentally verified by Z-scan measurements and excitation power dependence in transient absorption. Comparison of transient absorption spectra under one-photon and simultaneous two-photon excitation conditions revealed that the closed-ring isomer of mt-fDAE populated into higher excited states deactivates following three pathways on a timescale of ca. 200 fs: (i) the cycloreversion reaction more efficient than that by the one-photon process, (ii) internal conversion into the S_1 state, and (iii) relaxation into a lower state (S_1' state) different from the S_1 state. Time-resolved fluorescence measurements demonstrated that this S_1' state is relaxed to the S_1 state with the large emission probability. These findings obtained in the present work contribute to extension of the ON–OFF switching capability of fDAE to the biological window and application to super-resolution fluorescence imaging in a two-photon manner.

Graphical Abstract

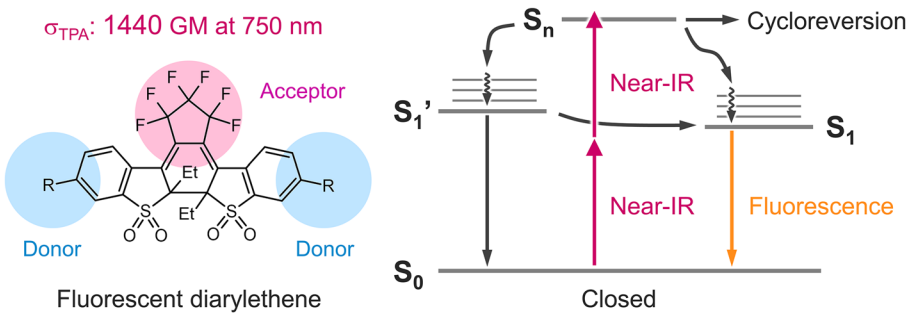

Keywords Photochromism · Diarylethene · Two-photon absorption · Excited state dynamics · Ultrafast spectroscopy

✉ Hikaru Sotome
sotome@laser.chem.es.osaka-u.ac.jp

✉ Masahiro Irie
iriem@rikkyo.ac.jp

✉ Hiroshi Miyasaka
miyasaka@chem.es.osaka-u.ac.jp

[1] Division of Frontier Materials Science and Center for Advanced Interdisciplinary Research, Graduate School of Engineering Science, Osaka University, Toyonaka, Osaka 560-8531, Japan

[2] Nanomaterials Research Institute (NMRI), National Institute of Advanced Industrial Science and Technology (AIST), Ikeda, Osaka 563-5877, Japan

[3] Department of Chemistry, Graduate School of Science and Technology, Kwansei Gakuin University, Sanda, Hyogo 669-1330, Japan

[4] Department of Chemistry and Research Center for Smart Molecules, Rikkyo University, 3-34-1 Nishi-Ikebukuro, Toshima-Ku, Tokyo 171-8501, Japan

Published online: 07 May 2024

Scheme. 1 Photochromic reaction of a typical fluorescent diarylethene derivative (fDAE)

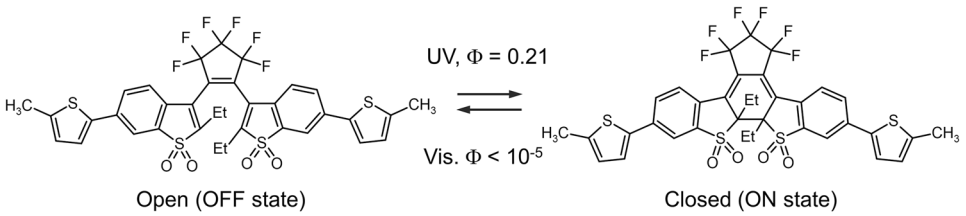

1 Introduction

Photochromism in molecular systems is defined as photoinduced reversible transformation between two chemical species [1–3]. Light irradiation pumps up one isomer into the electronic excited state, and the making and breaking of chemical bonds therein lead to the production of the other isomer on femtosecond and picosecond timescales. This ultrafast reaction behavior is a central mechanism in instantaneous change of chemical and physical properties in molecular photoswitches. Diarylethene (DAE) derivatives are an important class of photochromic molecules undergoing the 6π pericyclic reaction between the open- and closed-ring isomers [4–7]. Owing to their outstanding properties such as thermal stability and fatigue resistance, DAE derivatives have been widely utilized not only for photoswitching of molecular-level properties [8, 9] but also for macroscopic photomechanical responses in the field of materials science [10, 11].

Among a series of derivatives, DAE with sulfone units shows strong fluorescence in the closed-ring isomer and is recognized as turn-on mode fluorescent diarylethene derivatives (fDAE) [12–19], as shown in Scheme 1. Contrary to the closed-ring isomer with strong fluorescent property upon visible irradiation (ON state), the open-ring isomer is weakly fluorescent (OFF state). Thus, alternate ultraviolet and visible irradiation realizes ON–OFF switching of fluorescence, which can be applied to coordinate-targeted and coordinate-stochastic super-resolution microscopies such as RESOLFT and PALM [20–24]. The fine tuning of the photoswtiching efficiency by chemical modification fulfills the ON–OFF switching yields required for each imaging technique [18], and the derivatives with water solubility have successfully demonstrated a practical application to bioimaging [21].

In super-resolution fluorescence imaging, photofatigue of fluorescent dyes is, however, a critical issue for the long-term observation. The predominant origin of photofatigue is degradation of fluorescent compounds by photoirradiation in the shorter wavelength such as ultraviolet (UV) light. In addition, shorter penetration depth of tissues in the UV region hampers applications of molecular photoswitches to biological systems. Thus, photochromism driven by longer wavelength regions have been highly desirable in this context. For the enhancement of sensitivity in longer wavelength light and the suppression of the photofatigue effect, photochromism free from UV irradiation has been demonstrated on the basis of several methods such as higher order multiphoton (≥ 3) absorption by a near-infrared (NIR) laser pulse [25], photoexcitation of a weak absorption tail extending toward the longer wavelength (Urbach tail) [26, 27], singlet–triplet energy transfer in DAE-fluorophore dyads [28], photochromism induced by up-conversion based on triplet–triplet annihilation [29, 30] and stabilization of the excited state energy by charge transfer interaction [31].

We recently reported that a typical non-fluorescent diarylethene derivative has as a large two-photon absorption (TPA) cross-section as 380 GM at 730 nm and the off-resonant simultaneous TPA induces more efficient cycloreversion reaction in the higher excited state [32], which has been intensively studied by stepwise two-photon excitation for the past two decades [33–35]. Although relatively intense photoirradiation is required for simultaneous TPA, it can open a gated function for photochromism, that is, two-photon excitation by rather strong irradiation leads to the amplified reaction while weak irradiation does not induce any reaction. In this way, selecting the modes of photoexcitation enables us to control the photochromic reaction which is free from unexpected spontaneous reactions caused by background light. On the basis of these context and background, we have investigated the excited state dynamics of fDAE in the higher excited state attained by simultaneous TPA in the NIR region in the present work. The photochemical processes in higher excited states are a specific reaction behavior beyond the Kasha's rule and an intriguing aspect in time-resolved studies on chemical reaction dynamics [36, 37]. In addition, extension of the ON–OFF switching capability to the NIR region effectively suppresses photofatigue and leads to potential applications to super-resolution microscopy in the biological windows. In the following, we will discuss the TPA property, resultant dynamics in the higher excited states, and subsequent dynamics in the lower states of fDAE on the basis of time-resolved spectroscopies.

2 Experimental

2.1 Materials

1,2-Bis(2-ethyl-6-(5-methylthiophen-2-yl)-1-benzothiophene-1,1-dioxide-3-yl)perfluorocyclopentene (mt-fDAE, Scheme 1) was synthesized and purified as reported previously [16]. 1,4-Dioxane (Wako, infinity pure) was used as received. Before the measurements, continuous wave UV light was irradiated to the sample solution for conversion of the open-ring isomer into the closed-ring isomer. The cyclization and cycloreversion reaction yields are respectively 0.21 and $< 10^{-5}$ in 1,4-dioxane [16].

2.2 Transient absorption spectroscopy

Transient absorption spectra were measured with a home-built setup based on two optical parametric amplifiers (OPAs, TOPAS, Light Conversion) [38]. A Ti:Sapphire regenerative amplifier (Spectra-Physics, Spitfire, 802 nm, 1 mJ, 1 kHz, 100 fs) drove the overall system. The output was split into two parts and guided into the OPAs for generation of the excitation and probe beams. The outputs of the OPAs were, respectively, tuned to 750 and 1180 nm. The 750 nm pulse was used for excitation of the sample. The 1180 nm pulse was focused to a 2 mm CaF_2 plate and converted to white light continuum as the probe beam. This probe pulse was further divided into the signal and reference pulses. The signal pulse after passing through the sample cell and the reference one were detected by a pair of multichannel photodiode arrays (PMA10, Hamamatsu). The group velocity dispersion of the white light continuum was corrected on the basis of an optical Kerr signal of carbon tetrachloride. A time delay between the excitation and probe pulses was controlled with an optical delay stage. The irradiation of the excitation pulse was modulated with an optical chopper (Newport, 3501). Time resolution was evaluated as 150 fs by cross correlation measurement between the excitation and probe pulses. The sample solution was sealed into a rotation cell with an optical length of 2 mm, which was continuously rotated during the measurements to provide a fresh portion of the sample solution to the individual pulses. The contribution of simultaneous two-photon excitation of the open-ring isomer was negligibly small, as demonstrated in Fig. S1.

2.3 Fluorescence lifetime measurement

Fluorescence decay curves were measured using a time-correlated single photon counting (TCSPC) method [39]. The excitation light source was a Ti:Sapphire oscillator (Spectra-Physics, Tsunami, 1.7 W, 100 fs, 80 MHz) operating at the center wavelength of 800 nm. A small fraction of the output was picked up and detected for the starting pulse of TCSPC. The remaining major portion was irradiated to the sample after reducing the repetition rate to 8 MHz with an electro-optic modulator (Conoptics, Model 350). The fluorescence photons were spectrally discriminated by a monochromator (Acton, SP-2150), and collected with a photomultiplier tube (Hamamatsu, R3809U-50). The detected signal was sent to a TCSPC module (PicoQuant, PicoHarp 300). The polarization of the excitation pulse was set to the magic angle with respect to that of the fluorescence detection. For comparison, the same measurements were also performed under the excitation at 400 nm. The typical response time of the system was, respectively, determined to be 43 and 66 ps full width at half maximum for the excitations at 400 and 800 nm, by detecting the scattered photons from a colloidal solution.

2.4 Two-photon absorption spectral simulation

Two-photon absorption (TPA) spectrum was simulated based on the sum-over-state (SOS) formulation, reported elsewhere [40]. The molecular parameters for the simulation, i.e., transition energies, transition dipole moments, permanent dipole moments of the ground and excited states were obtained by the quantum chemical calculation at the CAM-B3LYP/6–31 + G(d) level with the Tamm–Dancoff approximation [41]. For the simulation 15 excited states were considered. The geometry optimization was carried out at the same level. Gaussian 16 software suite [42] was used for all quantum chemical calculations and the homemade procedure on Igor Pro was used to calculate the simulation spectra based on the SOS formulation.

3 Results and discussion

TPA properties of representative fluorescent diarylethene derivatives were investigated using quantum chemical calculations. Figure 1a shows HONTO (highest occupied natural transition orbital) and LUNTO (lowest unoccupied natural transition orbital) of the closed-ring isomer of mt-fDAE calculated at the CAM-B3LYP level using the 6–31 + G(d) basis set. A closer look reveals that HONTO is delocalized over the molecular framework while LUNTO is relatively located around the perfluorocyclopentene ring. Such an electronic structure, in which electron donor and acceptor are connected by π-electron systems, is advantageous for enhancement of TPA cross-Sect. [43]. Figure 1b shows simulated TPA spectra of the derivatives with different substituents at the molecular terminal positions together with one-photon absorption (OPA). Although the

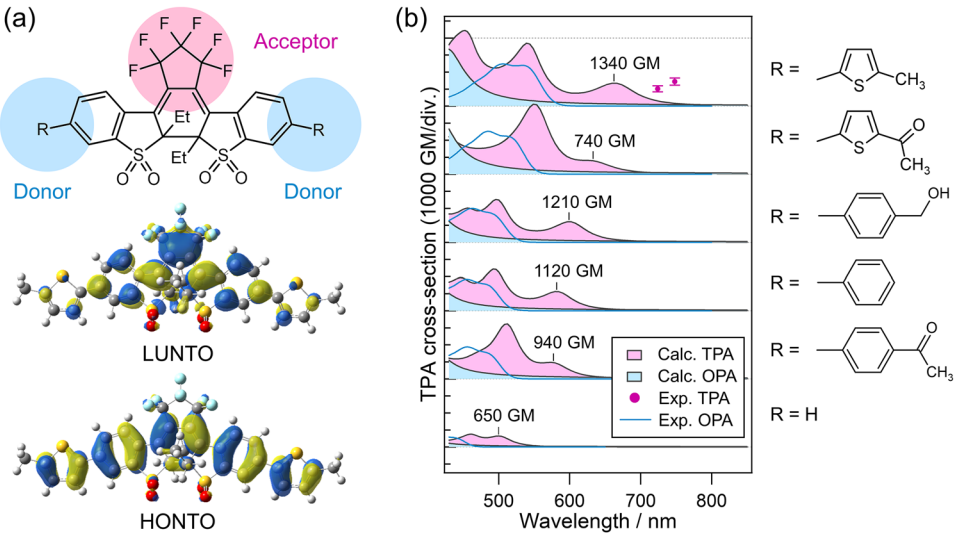

Fig. 1 **a** Electronic structure of fluorescent diarylethene derivatives and HONTO and LUNTO of mt-fDAE(c). **b** One-photon and two-photon absorption spectra of fluorescent diarylethene derivatives calculated at the CAM-B3LYP level using the 6–31 + G(d) basis set. The relaxation constants were set to 0.20 eV for the simulation. The experimental OPA data are also shown as cyan solid lines for comparison. TPA cross sections of mt-fDAE(c) experimentally determined are also shown

calculated OPA bands are systematically blue-shifted compared with the experimental ones, the spectral simulation qualitatively reproduced difference in the wavelength of absorption maximum over the derivatives with thiophene units, phenyl groups and no substituent. Among six derivatives, the closed-ring isomer with methylthiophene moieties show a TPA band around 660 nm and its tail extends up to the NIR window. It should be noted that a TPA cross-section of this derivative is larger than 1000 GM at the absorption maximum in the wavelength region > 600 nm. This calculation predicts that the fluorescent diarylethene derivative with methylthiophene moieties (mt-fDAE) has a rather large TPA cross-section. The origin of such a large cross-section is D-π-A-π-D structure, in which the methylthiophene and perfluorocyclopentene moieties, respectively, behave as electron donor and acceptor units. In the following section, we concentrate discussion to mt-fDAE because it is one of most typical derivatives and the excited state dynamics under the one-photon and stepwise two-photon excitation was already investigated in a previous report [44].

Steady-state absorption and fluorescence spectra of mt-fDAE in 1,4-dioxane solution are shown in Fig. 2. Open-ring isomer, mt-fDAE(o) has absorption only in the shorter wavelength region than 430 nm, while absorption of the closed-ring isomer, mt-fDAE(c), lies in the UV and visible regions. The absorption band of mt-fDAE(c) in the visible region corresponds to the transition to the lowest excited state where the one-photon cycloreversion reaction undergoes with a quite small reaction quantum yield < 10^{-5}. The fluorescence band of mt-fDAE(c) is peaked at ~ 590 nm with the Stokes shift of ca. 1800 cm^{-1}. Rather large shift is more or less affected by the moderate charge transfer character in the excited state, as observed in the solvent polarity dependence of the fluorescence spectrum of this system [45].

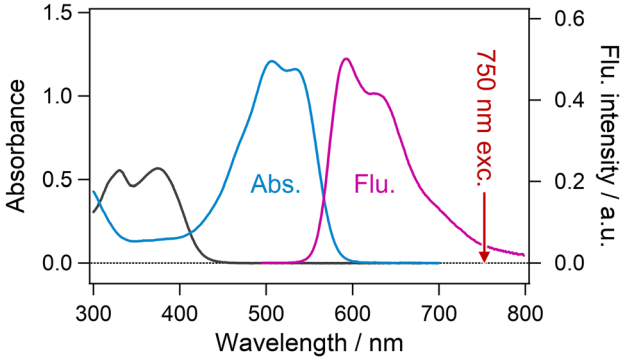

Fig. 2 Steady-state absorption and fluorescence spectra of mt-fDAE in 1,4-dioxane solution. Black and cyan curves show absorption of the open-ring and closed-ring isomers, respectively. A magenta curve shows fluorescence of the closed-ring isomer

Fluorescence quantum yield of mt-fDAE(c) was reported to be 0.78 in 1,4-dioxane solution [45].

To reveal the photoexcited dynamics starting in the higher excited state (S_n state), we applied transient absorption spectroscopy to mt-fDAE(c) under the simultaneous two-photon excitation condition. The excitation wavelength in this transient absorption spectroscopy was set to 750 nm, which is ca. 150 nm far from the one-photon absorption edge as shown in Fig. 2. Prior to detailed discussion on the spectral evolution, we show excitation power dependence of the transient absorption signals to ensure the simultaneous two-photon process taking place in this excitation condition. Figure 3a presents transient absorption spectra of mt-fDAE(c) in 1,4-dioxane solution at 10 ps after the excitation with various intensities, indicating that the spectral amplitude increases with an increase of the excitation power while keeping its band shape. For quantitative analysis, the transient absorption band integrated over 685–715 nm was

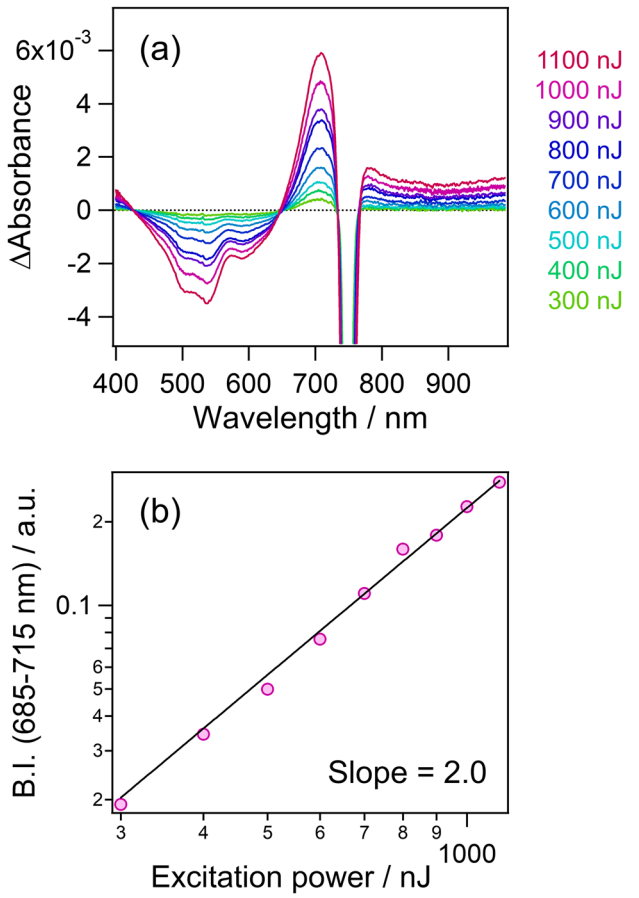

Fig. 3 **a** Transient absorption spectra of mt-fDAE(c) in 1,4-dioxane measured at various excitation powers. The excitation wavelength and delay time were, respectively, set to 750 nm and 10 ps. The signal around 750 nm was perturbed by scattering of the excitation pulse. **b** Excitation power dependence of the band integral in 685–715 nm

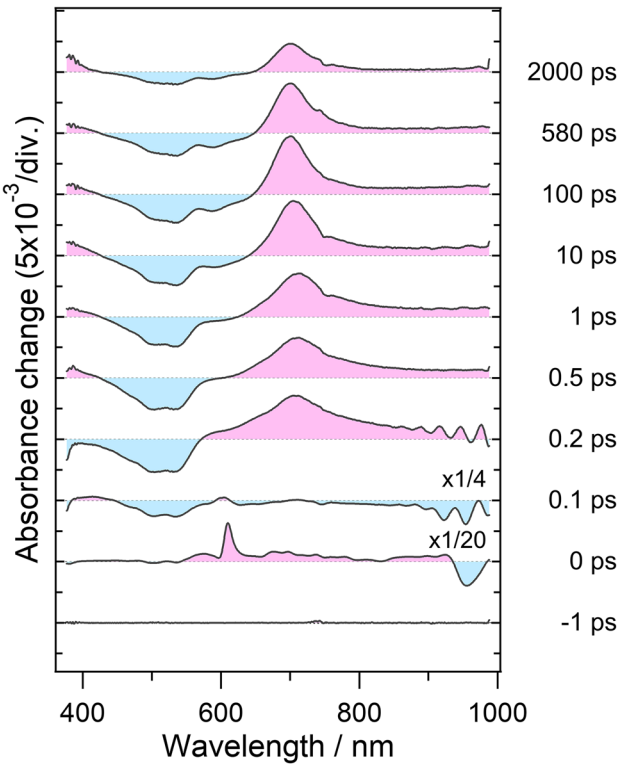

Fig. 4 Transient absorption spectra of mt-fDAE(c) in 1,4-dioxane excited with a femtosecond laser pulse at 750 nm. The excitation power was set to 650 nJ/pulse. The scattering of the excitation pulse and steady-state fluorescence from the sample were subtracted from all the spectra

plotted as a function of the excitation power in Fig. 3b. This power dependence shows a slope of ≈2.0, clearly indicating that the two-photon absorption initiates the excited state dynamics of the system. The Z-scan measurements determined the TPA cross-section of mt-fDAE(c) to be 1440 ± 210 GM (Figure S2), of which large value is consistent with the calculated results in Fig. 1b although the TPA band is likely to appear in the longer wavelength region than those predicted by the spectral simulation as well as the OPA process. Taken together with above results, we can safely conclude that the off-resonant simultaneous two-photon process is induced by pulsed irradiation at 750 nm.

Figure 4 shows time evolution of the transient absorption spectra of mt-fDAE(c) in 1,4-dioxane solution in the femtosecond to nanosecond time region. Although transient spectra at 0 and 0.1 ps are largely contaminated by stimulated Raman scattering and cross phase modulation due to solvent, the spectra at and after 0.2 ps are characterized by negative (< 570 nm) and positive (> 570 nm) bands. The negative band is ascribed to the ground state bleaching, which is similarly observed under the resonant one-photon excitation at 530 nm (Figure S3a) [44]. However, the spectrum at 0.2 ps has two different features in the wavelength region longer than 570 nm: (1) a negative band due to stimulated emission around 590 nm is almost absent and (2) the absorption band around 710 nm is rather broad, compared with the one-photon excitation condition. The first feature indicates that the two-photon-excited molecules are populated not in the fluorescent S_1 state but in the S_n state in the early stage after the excitation. That is, the broad positive band around 710 nm is ascribable to the S_n state although it may contain a portion of the vibrationally hot S_1 state, which is already produced through the internal conversion from the S_n state.

The stimulated emission band becomes prominent around 590 nm after 1 ps, indicating that the S_n state is relaxed into the S_1 state through internal conversion on a sub-picosecond timescale. In the time region later than 1 ps, this positive band undergoes a blue shift and spectral sharpening concomitantly with clear appearance of the stimulated emission band in 580–630 nm.

To precisely elucidate the excited state dynamics, we analyzed temporal evolution of transient absorbance. Figure 5

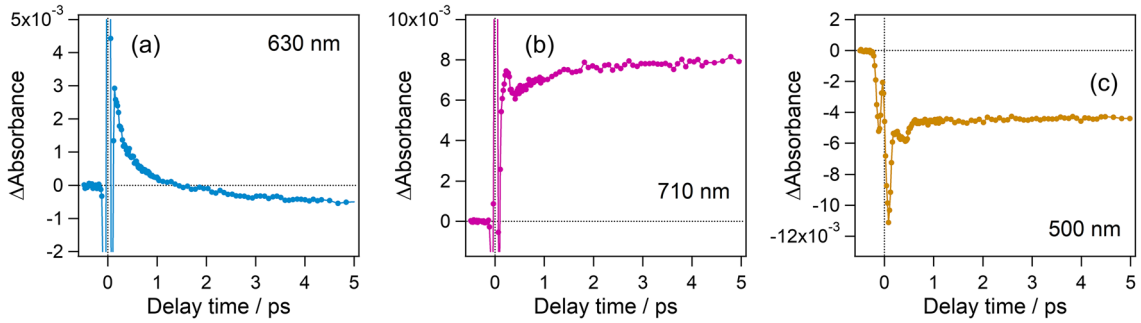

Fig. 5 Time profiles of transient absorbance of mt-fDAE(c) in 1,4-dioxane excited with a femtosecond laser pulse at 750 nm. The monitoring wavelengths are **a** 630 nm, **b** 710 nm and **c** 500 nm

shows time profiles of transient absorbance of mt-fDAE(c) monitored at three wavelength points. The time profile at 630 nm shows a biphasic evolution in the femtosecond and picosecond time regions. The first component corresponds to the increase of the stimulated emission. The subsequent decay at 630 nm and rise at 710 nm are associated with the blue shift and sharpening of the excited state absorption. This evolution is ascribed mainly to the cooling processes of the S_1 state. On the other hand, a marked evolution was not observed in the time profile at 500 nm where the ground state bleaching is dominant. This result indicates that the spectral evolution in the femtosecond and picosecond scales is mainly ascribable to the dynamical change within the excited state manifold. To comprehensively elucidate the dynamics, we applied global fitting analysis to this transient absorption data, of which results yielded decay-associated spectra (DAS) with the time constants of 240 fs and 10 ps in this time window (Figure S4). Also for transient absorption data under the one-photon excitation condition, DAS were derived for comparison with those under the two-photon excitation (Figure S3b and c). These two time constants, 240 fs and 10 ps, are, respectively, attributable to the lifetime of the S_n state and vibrational cooling and solvation in the S_1 state.

To precisely evaluate the dynamics specific to the simultaneous two-photon excitation, we compared the spectra observed under one-photon and two-photon excitation conditions. Figure 6 shows transient absorption spectra of mt-fDAE(c) in 1,4-dioxane solution excited with a femtosecond laser pulse at 530, 630 and 750 nm. The irradiations at 530 and 750 nm, respectively, correspond to the resonant one-photon and off-resonant two-photon excitation. Although the photoexcitation at 630 nm is apparently off-resonant with one-photon excitation, the absorption tail of the closed-ring form extends toward the longer wavelength with a rather small absorption coefficient (Urbach tail). Hence, the irradiation at 630 nm may also induce one-photon absorption from the vibrationally hot ground state. That is, one-photon absorption could take place in competition with two-photon

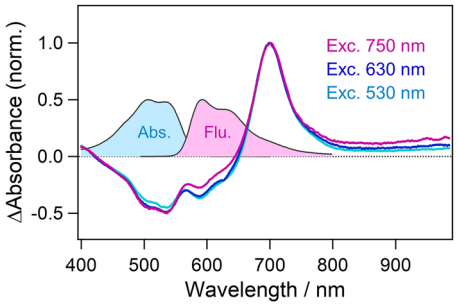

Fig. 6 Transient absorption spectra of mt-fDAE(c) in 1,4-dioxane monitored at 50 ps. The excitation wavelength was set to 530, 630 and 750 nm. Each spectrum was normalized at the absorption maximum wavelength of 700 nm. Steady-state absorption and fluorescence spectra are also shown for comparison

process under this excitation condition. The delay time was set to 50 ps, at which the vibrational cooling is fully completed and the excited molecule is thermally in equilibrium. These spectra were normalized at the absorption maximum wavelength of 700 nm. It is worth mentioning that the spectrum under the two-photon excitation at 750 nm shows a slightly larger bleaching signal of the ground state in 420–550 nm. This signal is a signature suggesting the efficient cycloreversion reaction in the S_n state, which will be discussed in detail in the later section. In the wavelength region longer than 550 nm, the spectrum is characterized by smaller signals of stimulated emission in 550–670 nm and a larger positive band in > 750 nm, compared with the one-photon excitation. These differences indicate that the internal conversion from the S_n state produces another lower excited state (S_1' state) except for the S_1 state.

To elucidate the S_1' state more clearly, we measured fluorescence time profiles under the simultaneous two-photon excitation condition. Figure 7 shows fluorescence decay curves of mt-fDAE(c) in 1,4-dioxane under one-photon (400 nm) and two-photon (800 nm) excitation conditions. Although a very small deviation remains around 0 ns [46], the fluorescence time profile under the one-photon excitation

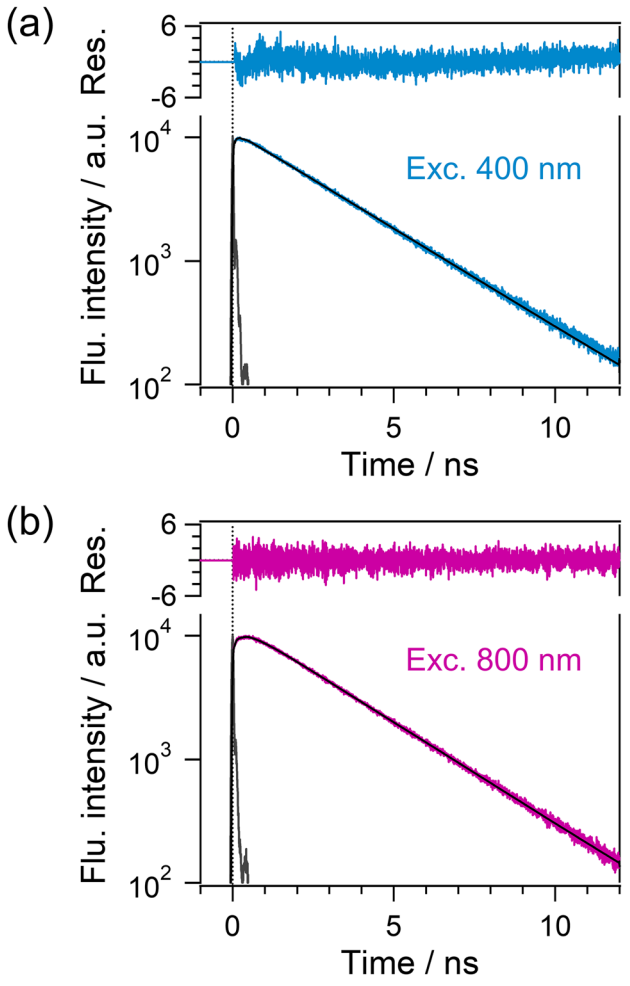

Fig. 7 Fluorescence time profiles of mt-fDAE(c) in 1,4-dioxane under **a** one-photon excitation at 400 nm and **b** two-photon excitation at 800 nm. The excitation powers were respectively set to 2 pJ for 400 nm excitation and 5 nJ for 800 nm excitation. The obtained time constants were 2.7 ns for (**a**), and 400 ps (rise) and 2.6 ns (decay) for (**b**)

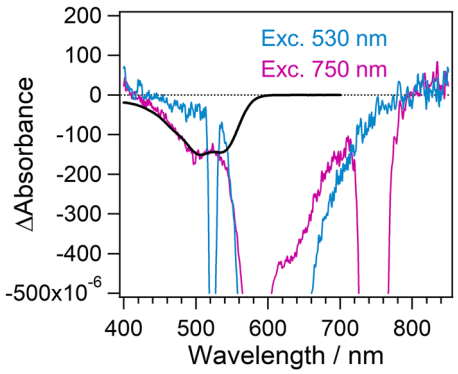

Fig. 8 Transient absorption spectra of mt-fDAE(c) in 1,4-dioxane monitored at 20 ns. The excitation wavelengths were set to 530 and 750 nm. Inversion of the steady-state absorption spectrum is also shown for comparison. The transient signal in the longer wavelength than 540 nm was contaminated by strong fluorescence from the sample in both the conditions

at 400 nm shows the monophasic decay with the lifetime of 2.7 ns, which is consistent with that in a previous report [16]. On the other hand, the decay curve under the two-photon excitation was not well fitted with a single component but it was fully reproduced with a double-exponential function with time constants of 400 ps (rise) and 2.6 ns (See details in Figure S5). The latter time constant (2.6 ns) is identical to the fluorescence lifetime of the S_1 state obtained under the one-photon excitation (2.7 ns) within experimental errors. This result indicates that the S_1' state is less fluorescent at this wavelength. The 400-ps rise component specific to the two-photon excitation indicates that the fluorescent S_1 state is gradually produced from the dark S_1' state with the time constant of 400 ps although a remaining portion of the S_1 state is produced from the S_n state in the femtosecond time region. Actually, global fitting analysis using four time constants of 240 fs, 10 ps, 400 ps (fixed) and 2.6 ns (fixed) well reproduced the transient absorption data in the wide time region. The DAS with the 400-ps time constant shows positive and negative signals around 580 and 690 nm (Figure S4). In general, a positive sign in the DAS indicates an absorption decay of transient species and increases of the stimulated emission while a negative one indicates the recovery of negative bands due to the ground state bleaching and stimulated emission, and increase of a newly appearing species. In the present case, these signals, respectively, correspond to the increase of the stimulated emission and the S_1 state absorption, ensuring the interconversion from the S_1' state to the S_1 state. In addition, the 400-ps DAS shows a small negative band in the wavelength of the ground state bleaching (450–550 nm), implying that a fraction of the S_1' state is directly deactivated into the S_0 state. Summarizing above results and discussion, the dark S_1' is produced from the S_n state produced by the two-photon excitation in NIR regions and mainly undergoes the conversion into the S_1 state and deactivation to the S_0 state.

As discussed above, highly excited state of mt-fDAE pumped by simultaneous two-photon excitation in NIR region undergoes cycloreversion reaction, relaxation to the specific S_1' state in competition with the S_1 state formation. To quantitatively estimate the cycloreversion reaction yield in the S_n state pumped by the simultaneous two-photon absorption, we measured the permanent bleaching signal due to the cycloreversion reaction. Figure 8 shows transient absorption spectra of mt-fDAE(c) in 1,4-dioxane monitored at 20 ns, at which almost all the population of the excited state returns back to the ground state. No permanent bleaching remains by the one-photon excitation (530 nm), indicating that the cycloreversion or the intersystem processes are negligibly small from the S_1 state with the lifetime of 2.7 ns.

Also under the two-photon excitation condition (750 nm), no positive band survives, indicating that long-lived species such as the triplet state is not present as well as the one-photon process. On the other hand, the permanent bleaching signal was observed in the wavelength region shorter than 550 nm under the two-photon excitation condition. This bleaching signal corresponds to the cycloreversion reaction. From ΔAbsorbance, the molar absorption coefficient at 530 nm, and the concentration of mt-fDAE, the conversion from the closed-ring isomer into the open-ring isomer was calculated to be 0.037% of mt-fDAE in the irradiation spot. On one hand, the excitation portion by the two-photon absorption was estimated to be 4.4% of the ground state molecules from the TPA cross-section and irradiation condition (see details in the Supplementary Information). From these values, we quantitatively estimated the cycloreversion quantum yield in the S_n state to be 8.5×10^{-3}, which is much larger than the one-photon reaction quantum yield of $< 10^{-5}$ at least by a factor of ca. 1000.

Figure 9 illustrates the excited state dynamics of mt-fDAE(c) by the simultaneous two-photon excitation at 750 nm. Closed-ring isomer of mt-fDAE is efficiently excited to the S_n state in the simultaneous two-photon manner owing to the large two-photon cross-section of 1440 GM. This S_n state is relaxed into the fluorescent S_1 and dark S_1' states on a timescale of ca. 200 fs and undergoes the subsequent cooling process therein. The branching ratio to the S_1' and S_1 states was estimated to be 0.22: 0.78 from kinetics analysis based on the fluorescence rise and decay in Fig. 7b, the details of which are shown in the Supplementary Information (Sect. 7). A major portion of this S_1' state is converted to the fluorescent S_1 state with the time constant of 400 ps. Although the character of this dark S_1' state remains elusive due to the spectrally silent property, such a relatively long-lived intermediate has been also reported in a previous study on the two-photon cycloreversion dynamics of a non-fluorescent diarylethene derivative [32]. According to this work, the lower excited state, which is produced not by one-photon excitation but by simultaneous two-photon excitation, is a non-reactive species and does not contribute to the efficient cycloreversion reaction specific to the two-photon excitation. Considering the above insights and relatively longer lifetime as photoisomerization molecules, we tentatively conclude that the efficient cycloreversion reaction proceeds directly through the S_n state with the quantum yield of 8.5×10^{-3} before the relaxation into the S_1' state. This issue will be approached by direct detection of the product formation with time-resolved vibrational spectroscopy, as we have reported for the one-photon cycloreversion reaction of a non-fluorescent diarylethene derivative [47].

4 Conclusion

We investigated the excited state dynamics of mt-fDAE(c) in the S_n state attained by the off-resonant simultaneous two-photon excitation. The quantum chemical calculation and Z-scan measurements confirmed that mt-fDAE(c) has high TPA property (1440 GM at 750 nm) and is a promising TPA material with fluorescence ON–OFF switching capability. The S_n state populated by the simultaneous two-photon excitation undergoes the efficient cycloreversion reaction with the quantum yield of 8.5×10^{-3}, which corresponds to at least ca. 10^3 times reaction enhancement. Behind this amplified reaction, other portion of the S_n state undergoes the parallel relaxation into the fluorescent S_1 state and dark S_1' state. The S_1' state is subsequently relaxed into the S_1 state in several hundreds of picoseconds. These results in the present study not only contribute to understanding of elementary processes in the high-lying excited state but also provide fundamentals toward the application of molecular photoswitches to super-resolution fluorescence imaging and biological systems in the NIR window.

Supplementary Information The online version contains supplementary material available at https://doi.org/10.1007/s43630-024-00573-y.

Acknowledgements This work was partly supported by JSPS KAKENHI Grant Numbers JP21H01888, JP22H00331, JP21H05395,

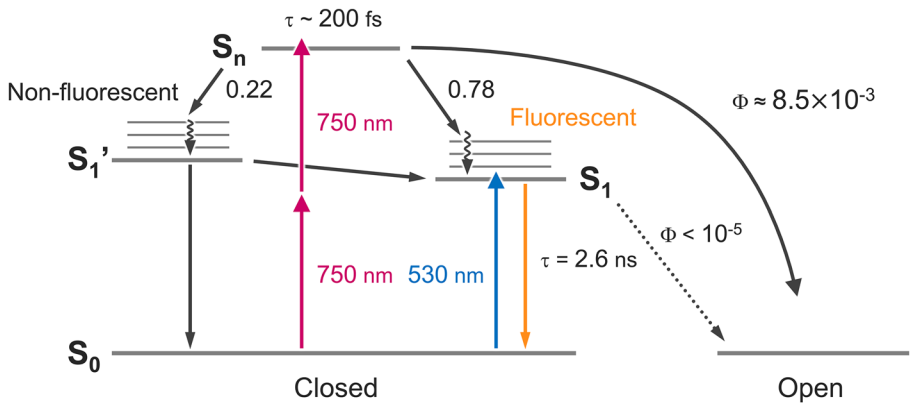

Fig. 9 Overall scheme of the excited state dynamics of mt-fDAE(c) induced by off-resonant simultaneous two-photon absorption

JP23H03956, JP23H01926, JP23H04877 to H. S., JP26107002, JP21H01889, JP21K18934 to H. M., JP26107004, JP23K04710 to K. K., and JP15H01096, JP17H05272 to M. M.

Funding Open Access funding provided by Osaka University.

Data availability The data that support the findings of the present study are available from the corresponding authors upon reasonable request.

Declarations

Conflict of interest The authors declare no conflict of interest.

References

1. Dürr, H., & Bouas-Laurent, H. (1990). *Photochromism molecules and systems*. Elsevier.
2. Feringa, B. L. (2001). *Molecular switches*. Wiley-VCH.
3. Irie, M., Yokoyama, Y., & Seki, T. (2013). *New Frontiers in photochromism*. Springer.
4. Irie, M., & Mohri, M. (1988). Thermally irreversible photochromic systems. reversible photocyclization of diarylethene derivatives. *Journal of Organic Chemistry, 53*, 803–808.
5. Irie, M. (2000). Diarylethenes for memories and switches. *Chemical Reviews, 100*, 1685–1716.
6. Irie, M., Fukaminato, T., Matsuda, K., & Kobatake, S. (2014). Photochromism of diarylethene molecules and crystals: memories, switches, and actuators. *Chemical Review, 14*, 12174–12277.
7. Irie, M. (2021). *Diarylethene Molecular Photoswitches: Concepts and Functionalities*. Wiley-VCH.
8. Irie, M., Fukaminato, T., Sasaki, T., Tamai, N., & Kawai, T. (2002). A digital fluorescent molecular photoswitch. *Nature, 420*, 759–760.
9. Matsuda, K., & Irie, M. (2000). A diarylethene with two nitronyl nitroxides: photoswitching of intramolecular magnetic interaction. *Journal of the American Chemical Society, 122*, 7195–7201.
10. Kobatake, S., Takami, S., Muto, H., Ishikawa, T., & Irie, M. (2007). Rapid and reversible shape changes of molecular crystals on photoirradiation. *Nature, 446*, 778–781.
11. Morimoto, M., & Irie, M. (2010). A diarylethene cocrystal that converts light into mechanical work. *Journal of the American Chemical Society, 132*, 14172–14178.
12. Jeong, Y. C., Yang, S. I., Ahn, K. H., & Kim, E. (2005). Highly fluorescent photochromic diarylethene in the closed-ring form. *Chemical Communications, 19*, 2503–2505.
13. Jeong, Y. C., Yang, S. I., Kim, E., & Ahn, K. H. (2006). Development of highly fluorescent photochromic material with high fatigue resistance. *Tetrahedron, 62*, 5855–5861.
14. Jeong, Y. C., Park, D. G., Lee, I. S., Yang, S. I., & Ahn, K. H. (2009). Highly fluorescent photochromic diarylethene with an excellent fatigue property. *Journal of Materials Chemistry, 19*, 97–103.
15. Gillanders, F., Giordano, L., Díaz, S. A., Jovin, T. M., & Jares-Erijman, E. A. (2014). Photoswitchable fluorescent diheteroarylethenes: substituent effects on photochromic and solvatochromic properties. *Photochemical and Photobiological Sciences, 13*, 603–612.
16. Uno, K., Niikura, H., Morimoto, M., Ishibashi, Y., Miyasaka, H., & Irie, M. (2011). In situ preparation of highly fluorescent dyes upon photoirradiation. *Journal of the American Chemical Society, 133*, 13558–13564.
17. Sumi, T., Kaburagi, T., Morimoto, M., Une, K., Sotome, H., Ito, S., Miyasaka, H., & Irie, M. (2015). Fluorescent photochromic diarylethene that turns on with visible light. *Organic Letters, 17*, 4802–4805.
18. Takagi, Y., Morimoto, M., Kashihara, R., Fujinami, S., Ito, S., Miyasaka, H., & Irie, M. (2017). Turn-on mode fluorescent diarylethenes: control of the cycloreversion quantum yield. *Tetrahedron, 73*, 4918–4924.
19. Irie, M., & Morimoto, M. (2018). Photoswitchable turn-on mode fluorescent diarylethenes: strategies for controlling the switching response. *Bulletin of the Chemical Society of Japan, 91*, 237–250.
20. Roubinet, B., Bossi, M. L., Alt, P., Leutenegger, M., Shojaei, H., Schnorrenberg, S., Nizamov, S., Irie, M., Belov, V. N., & Hell, S. W. (2016). Caboxylated photoswitchable diarylethenes for biolabeling and super-resolution RESOLFT microscopy. *Angewandte Chemie International Edition, 55*, 15429–15433.
21. Roubinet, B., Weber, M., Shojaei, H., Bates, M., Bossi, M. L., Belov, V. N., Irie, M., & Hell, S. W. (2017). Fluorescent photoswitchable diarylethenes for biolabeling and single-molecule localization microscopies with optical superresolution. *Journal of the American Chemical Society, 139*, 6611–6620.
22. Uno, K., Bossi, M. L., Konen, T., Belov, V. N., Irie, M., & Hell, S. W. (2019). Asymmetric diarylethenes with oxidized 2-alkylbenzothiophen-3-yl units: chemistry, fluorescence, and photoswitching. *Advanced Optical Materials, 7*, 1801746.
23. Uno, K., Bossi, M. L., Irie, M., Belov, V. N., & Hell, S. W. (2019). Reversibly photoswitchable fluorescent diarylethenes resistant against photobleaching in aqueous solutions. *Journal of the American Chemical Society, 141*, 16471–16478.
24. Uno, K., Aktalay, A., Bossi, M. L., Irie, M., Belov, V. N., & Hell, S. W. (2021). Turn-on mode diarylethenes for bioconjugation and fluorescence microscopy of cellular structures. *Proceedings of the National Academy of Sciences of the United States of America, 118*, e2100165118.
25. Mori, K., Ishibashi, Y., Matsuda, H., Ito, S., Nagasawa, Y., Nakagawa, H., Uchida, K., Yokojima, S., Nakamura, S., Irie, M., & Miyasaka, H. (2011). One-color reversible control of photochromic reactions in a diarylethene derivative: three-photon cyclization and two-photon cycloreversion by a near-infrared femtosecond laser pulse at 1.28 μm. *Journal of the American Chemical Society, 133*, 2621–2625.
26. Arai, Y., Ito, S., Fujita, H., Yoneda, Y., Kaji, T., Takei, S., Kashihara, R., Morimoto, M., Irie, M., & Miyasaka, H. (2017). One-colour control of activation, excitation and deactivation of a fluorescent diarylethene derivative in super-resolution microscopy. *Chemical Communications, 53*, 4066–4069.
27. Kashihara, R., Morimoto, M., Ito, S., Miyasaka, H., & Irie, M. (2017). Fluorescence photoswitching of a diarylethene by irradiation with single-wavelength visible light. *Journal of the American Chemical Society, 139*, 16498–16501.
28. Ikariko, I., Kim, S., Hiroyasu, Y., Higashiguchi, K., Matsuda, K., Hirose, T., Sotome, H., Miyasaka, H., Yokojima, S., Irie, M., Kurihara, S., & Fukaminato, T. (2022). All-visible (>500 nm)-light-induced diarylethene photochromism based on multiplicity

conversion via intramolecular energy transfer. *Journal of Physical Chemistry Letters, 13*, 7429–7436.
29. Larsson, W., Morimoto, M., Irie, M., Andréasson, J., Albinsson, B. (2023). Diarylethene isomerization by using triplet–triplet annihilation photon upconversion. *Chemistry: A European Journal*, *29*, e202203651.
30. Tokunaga, A., Uriarte, L. M., Mutoh, K., Fron, E., Hofkens, J., Sliwa, M., & Abe, J. (2019). Photochromic reaction by red light via triplet fusion upconversion. *Journal of the American Chemical Society, 141*, 17744–17753.
31. Kometani, A., Inagaki, Y., Mutoh, K., & Abe, J. (2020). Red or near-infrared light operating negative photochromism of a binaphthyl-bridged imidazole dimer. *Journal of the American Chemical Society, 142*, 7995–8005.
32. Sotome, H., Nagasaka, T., Une, K., Okui, C., Ishibashi, Y., Kamada, K., Kobatake, S., Irie, M., & Miyasaka, H. (2017). Efficient cycloreversion reaction of a diarylethene derivative in higher excited states attained by off-resonant simultaneous two-photon absorption. *Journal of Physical Chemistry Letters, 8*, 3272–3276.
33. Miyasaka, H., Murakami, M., Itaya, A., Guillaumont, D., Nakamura, S., & Irie, M. (2001). Multiphoton gated photochromic reaction in a diarylethene derivative. *Journal of the American Chemical Society, 123*, 753–754.
34. Murakami, M., Miyasaka, H., Okada, T., Kobatake, S., & Irie, M. (2004). Dynamics and mechanisms of the multiphoton gated photochromic reaction of diarylethene derivatives. *Journal of the American Chemical Society, 126*, 14764–14772.
35. Sotome, H., Nagasaka, T., Une, K., Morikawa, S., Katayama, T., Kobatake, S., Irie, M., & Miyasaka, H. (2017). Cycloreversion reaction of a diarylethene derivative at higher excited states attained by two-color, two-photon femtosecond pulsed excitation. *Journal of the American Chemical Society, 139*, 17159–17167.
36. Demchenko, A. P., Tomin, V. I., & Chou, P.-T. (2017). Breaking the Kasha rule for more efficient photochemistry. *Chemical Reviews, 117*, 13353–13381.
37. del Valle, J. C., & Catalán, J. (2019). Kasha's rule: a reappraisal. *Physical Chemistry Chemical Physics, 21*, 10061–10069.
38. Sotome, H., Kitagawa, D., Nakahama, T., Ito, S., Kobatake, S., Irie, M., & Miyasaka, H. (2019). Cyclization reaction dynamics of an inverse type diarylethene derivative as revealed by time-resolved absorption and fluorescence spectroscopies. *Physical Chemistry Chemical Physics, 21*, 8623–8632.
39. Nagasawa, Y., Itoh, T., Yasuda, M., Ishibashi, Y., Ito, S., & Miyasaka, H. (2008). Ultrafast charge transfer process of 9,9'-bianthryl in imidazolium ionic liquids. *Journal of Physical Chemistry B, 112*, 15758–15765.
40. Ohta, K., Yamada, S., Kamada, K., Slepkov, A. D., Hegmann, F. A., Tykwinski, R. R., Shirtcliff, L. D., Haley, M. M., & Sałek, P. (2011). Two-photon absorption properties of two-dimensional π-conjugated chromophores: combined experimental and theoretical study. *Journal of Physical Chemistry A, 115*, 105–117.
41. Hirata, S., & Head-Gordon, M. (1999). Time-dependent density functional theory within the Tamm-Dancoff approximation. *Chemical Physics Letters, 314*, 291–299.
42. Gaussian 16, Revision C.01, Frisch, M. J., Trucks, G. W., Schlegel, H. B., Scuseria, G. E., Robb, M. A., Cheeseman, J. R., Scalmani, G., Barone, V., Petersson, G. A., Nakatsuji, H., Li, X., Caricato, M., Marenich, A. V., Bloino, J., Janesko, B. G., Gomperts, R., Mennucci, B., Hratchian, H. P., Ortiz, J. V., Izmaylov, A. F., Sonnenberg, J. L., Williams-Young, D., Ding, F., Lipparini, F., Egidi, F., Goings, J., Peng, B., Petrone, A., Henderson, T., Ranasinghe, D., Zakrzewski, V. G., Gao, J., Rega, N., Zheng, G., Liang, W., Hada, M., Ehara, M., Toyota, K., Fukuda, R., Hasegawa, J., Ishida, M., Nakajima, T., Honda, Y., Kitao, O., Nakai, H., Vreven, T., Throssell, K., Montgomery, J. A., Jr., Peralta, J. E., Ogliaro, F., Bearpark, M. J., Heyd, J. J., Brothers, E. N., Kudin, K. N., Staroverov, V. N., Keith, T. A., Kobayashi, R., Normand, J., Raghavachari, K., Rendell, A. P., Burant, J. C., Iyengar, S. S., Tomasi, J., Cossi, M., Millam, J. M., Klene, M., Adamo, C., Cammi, R., Ochterski, J. W., Martin, R. L., Morokuma, K., Farkas, O., Foresman, J. B., Fox, D. J. Gaussian, Inc., Wallingford CT, 2016.
43. Albota, M., Beljonne, D., Brédas, J.-L., Ehrlich, J. E., Fu, J.-Y., Heikal, A. A., Hess, S. E., Kogej, T., Levin, M. D., Marder, S. R., McCord-Maughon, D., Perry, J. W., Röckel, H., Rumi, M., Subramaniam, G., Webb, W. W., Wu, X.-L., & Xu, C. (1998). Design of organic molecules with large two-photon absorption cross sections. *Science, 281*, 1653–1656.
44. Nagasaka, T., Kunishi, T., Sotome, H., Koga, M., Morimoto, M., Irie, M., & Miyasaka, H. (2018). Multiphoton-gated cycloreversion reaction of a fluorescent diarylethene derivative as revealed by transient absorption spectroscopy. *Physical Chemistry Chemical Physics, 20*, 19776–19783.
45. Morimoto, M., Takagi, Y., Hioki, K., Nagasaka, T., Sotome, H., Ito, S., Miyasaka, H., & Irie, M. (2018). A turn-on mode fluorescent diarylethene: Solvatochromism of fluorescence. *Dyes and Pigments, 153*, 144–149.
46. A very small deviation from the fitting curve around 0 ns in Figure 7a may originate from fluorescence from the vibrationally hot S_1 state and/or the instrumental response function affected by a color effect of the photomultiplier tube, that is, wavelength-dependent timing characteristics.
47. Sotome, H., Okajima, H., Nagasaka, T., Tachii, Y., Sakamoto, A., Kobatake, S., Irie, M., & Miyasaka, H. (2020). Geometrical evolution and formation of the photoproduct in the cycloreversion reaction of a diarylethene derivative probed by vibrational spectroscopy. *ChemPhysChem, 21*, 1524–1530.